FEBS Letters 580 (2006) 6083–6092

Pfnek3: An atypical activator of a MAP kinase in *Plasmodium falciparum*

Yu Min Lye, Maurice Chan, Tiow-Suan Sim*

Department of Microbiology, Yong Loo Lin School of Medicine, National University of Singapore, MD4A, 5 Science Drive 2, Singapore 117597, Republic of Singapore

Received 17 July 2006; revised 13 September 2006; accepted 4 October 2006

Available online 12 October 2006

Edited by Francesc Posas

Abstract The canonical mitogen-activated protein kinase (MAPK) signal cascade was previously suggested to be atypical in the malaria parasite. This raises queries on the existence of alternative mediators of plasmodial MAPK pathways. This study describes, Pfnek3, a malarial protein kinase belonging to the NIMA (Never in Mitosis, *Aspergillus*) family. Endogenous Pfnek3 is expressed during late asexual to gametocyte stages and lacks some classical protein kinase sequence motifs. Moreover, Pfnek3 is phylogenetically distant from mammalian NIMA-kinases. Recombinant Pfnek3 was able to phosphorylate and stimulate a malarial MAPK (Pfmap2). Contrastingly, this was not observed with two other kinases, Pfmap1 and human MAPK1, suggesting that the Pfnek3–Pfmap2 interaction may be specific for Pfmap2 regulation. In summary, our data reveal a malarial NIMA-kinase with the potential to regulate a MAPK. Possessing biochemical properties divergent from classical mammalian NIMA-kinases, Pfnek3 could potentially be an attractive target for parasite-selective anti-malarials.

Keywords: Malaria; *Plasmodium*; Protein kinase; Erythrocytic-stage

1. Introduction

Plasmodium falciparum is responsible for the most lethal form of human malaria. Currently, reports of widespread re-emergence of drug resistance exacerbate the problem [1]. To date, the development of effective vaccines has yet to produce significant success. Therefore, a more detailed understanding of parasite development and growth may be vital in fortifying our molecular arsenal against the disease. The malaria life cycle is appreciably complex [2]. Briefly, the sporozoites target the liver upon inoculation by the mosquito vector and develop into asexual forms that infect red blood cells specifically. During the asexual intraerythrocytic stage, some parasites develop into gametocytes which are picked up by another feeding mosquito. In the mosquito midgut, the gametocytes fuse and form zygotes that escape the midgut and transform into sporozoites that migrate to the vector's salivary glands, ready to infect a new host. Surprisingly, the signaling mechanisms throughout the entire developmental process are poorly understood. It has been established in other eukaryotic cells that molecular signaling is a key to a cell's fate. Therefore, it is reasonable to suggest that signal transduction control is essential to parasite growth. A methodical approach to unveil these pathways may therefore lead to the identification of important signaling mediators.

We are interested in understanding the role of protein kinase pathways in the malaria parasite. Among eukaryotes, protein kinases belonging to the mitogen-activated protein kinase superfamily (MAPK, also called ERK, extracellularly regulated kinase) are currently among the best understood. MAPKs are believed to be highly conserved among eukaryotes and are central to the transduction of extracellular mitogenic stimuli down a cascade of ATP-dependent protein kinases. Two copies of *P. falciparum* MAPKs (Pfmap1 and Pfmap2) have been identified so far [3,4]. Both MAPKs share a peptide sequence identity of 41% in their catalytic domain. Phosphorylation of a threonine–tyrosine (TXY) sequence motif by an upstream kinase is usually needed for the activation of classical MAPKs. The TXY motif is completely conserved in Pfmap1 as TDY (PlasmoDB identifier: PF14_0294), and is evolutionarily altered to TSH in Pfmap2 (PlasmoDB identifier: PF11_0147). Pbmap2, the *Plasmodium berghei* counterpart of Pfmap2 was recently demonstrated to regulate gametogenesis via gene-disruption studies as well as in sex-specific proteomic analyses [5,6].

To further understand molecular mechanisms regulating the development of the parasite, protein kinase genes highly-expressed in gametocytes were strategically identified from transcriptome data deposited in PlasmoDB.org, and cloned for biochemical characterization. The result of data-mining revealed four *Plasmodium* genes clustered as sequences with homology to the NIMA (Never in Mitosis, *Aspergillus*) protein kinase family [7]. Of these four genes, three were revealed by microarray data to be expressed predominantly in gametocytes [8,9]. The founding member of the NEK family, NIMA, was described in *Aspergillus nidulans* and shown to be required for G2/M transition [10]. Thus far, other NIMA homologues have been identified in many eukaryotes, and there is growing evidence that NIMA-family kinases (NEKs) play the role of cell cycle regulators [11].

Numerous attempts have been made to identify candidate kinases upstream of Pfmap1 and Pfmap2. For example, it has previously been suggested that Pfnek1, a NIMA-family

*Corresponding author. Fax: +65 67766872.
E-mail address: micsimts@nus.edu.sg (T.-S. Sim).

Abbreviations: MAPK, mitogen-activated protein kinase; MAPKK, MAPK kinase; NIMA, never in mitosis, *Aspergillus*; NEK, NIMA-related kinase; Pfnek, *Plasmodium falciparum* NIMA-related kinase; Pfmap, *Plasmodium falciparum* MAP kinase; hMAPK1, human MAPK 1; GST, glutathione-S-transferase; MBP, myelin basic protein; FL, full-length; TR, truncated; PBS, phosphate buffered saline; BSA, bovine serum albumin; ELISA, enzyme-linked immunosorbent assay; WB, Western blot; Ctrl, control

0014-5793/$32.00
doi:10.1016/j.febslet.2006.10.003

kinase is an upstream regulator (i.e. MAPKK, also called MEK, MAPK/ERK Kinase) of Pfmap2 [12]. Unfortunately, bona fide in vivo activity of Pfnek1 was not established and recombinant Pfnek1 did not stimulate Pfmap1 [12]. A second protein kinase, PfPK7, with a MEK-like motif was reported [13]. Interestingly, its sequence similarity to MEKs is limited to the C-terminal domain while its N-terminal region bears similarity to PKAs (protein kinase A). In view of the above, and the fact that the malaria kinome reveals the lack of other MEK-coding DNA sequences [7], Dorin et al. suggested that a regular three-step MAP kinase cascade is possibly non-existent in the malaria parasite [13]. Thus, the existence of unusual signaling mediators that can regulate plasmodial MAPKs remains an intriguing question of *Plasmodium* biology.

The advent of the PlasmoDB repository (www.PlasmoDB.org) has eased our search for potential signaling mediators. Capitalizing on the transcriptome data offered in PlasmoDB [8,9], it was possible to identify a range of annotated gene products with expression profiles well-correlated with Pfmap1 and/or Pfmap2. We were intrigued by a sequence identified as PFL0080c (herein after referred to as *Pfnek3* following [7]), because it has an asexual intraerythrocytic expression profile akin to that of Pfmap1 whilst also being highly up-regulated during the gametocyte stage, where Pfmap2 is specifically expressed [4]. The results in this study demonstrate (i) the biochemical characterization of Pfnek3, (ii) the enhancement of Pfmap2 kinase activity by Pfnek3 and (iii) expression of Pfnek3 in the blood stages of the malaria parasite.

2. Materials and methods

2.1. Parasite cultures

The source of *P. falciparum* Tan strain was National University Hospital, Singapore. Parasite line 3D7 (MRA-102, MR4, ATCC Manassas Virginia) was a gift from MR4, the malaria resource repository (http://www.malaria.mr4.org/). The parasites were grown in human erythrocytes as described previously [14].

2.2. Molecular cloning and site-directed mutagenesis of Pfnek3 cDNA

Genomic DNA and total RNA were extracted from asynchronous cultures of intraerythrocytic *P. falciparum* (Tan and 3D7 strains) using the QIAamp® DNA Blood Mini Kit and RNeasy® Mini Kit, respectively (Qiagen, Germany). The Sensiscript® RT kit (Qiagen, Germany) was used to reverse-transcribe *Pfnek3* from a poly-A^+ mRNA-enriched template using a reverse primer, OL768, 5′-gaattcTTATTGAACCGTTATACAT-3′ (*Eco*RI site lowercase) for first strand synthesis prior to thermocycling. To verify the intron structure of the *Pfnek3* gene, PCR was performed on intraerythrocytic parasite genomic DNA using a pair of primers, (OL771) 5′-ggatccGTTTGCATTTACTTGTTTT-3′ (*Bam*HI site lowercase) and OL768 (sequence above).

As evident in other studies, the presence of N-terminal hydrophobic regions in a recombinant protein may interfere with subsequent expression in *Escherichia coli* [15]. Therefore, the truncated form of the *Pfnek3* gene encoding a peptide lacking the first 59 amino acids was amplified using another forward primer, (OL767) 5′-ggatccTGTGAGAAGAAATACCAGG-3′ (*Bam*HI site lowercase). All genes were amplified with *Pfu* DNA polymerase (Promega, USA) using thermocycling parameters previously described [16].

PCR and RT-PCR products were gel-purified and ligated onto the pCR-BluntII-TOPO™ (Invitrogen, USA). Positive constructs were verified by DNA sequencing. The cloned full-length and truncated *Pfnek3* sequences were thereafter named FL-*Pfnek3* and TR-*Pfnek3*, respectively. Mutant, 'kinase-dead' enzymes were constructed using the overlap extension protocol [17]. A K102M mutation was introduced at the kinase sub-domain II into the plasmid carrying TR-*Pfnek3* to generate a catalytically-inactive recombinant kinase (called ΔPfnek3). The primer pair used was (OL979) 5′-GAGATATATATCTatgGTATATGATATATATGG-3′ and (OL980) 5′-CCATATATATCATATACCATAGATATATATATCTC-3′. The plasmid carrying GST-Pfmap2 (a gift from C. Doerig, Wellcome Centre for Molecular Parasitology) was similarly mutated at K135 using (OL1138) 5′-CAAATAAAAATGTGGCTATAatgAAGGTTAATAG-3′ and (OL1139) 5′-CTATTAACCTTCATTATAGCCACATTTTTATTTG-3′.

2.3. Recombinant kinase production

FL-*Pfnek3*, TR-*Pfnek3* and TR-ΔPfnek3 fragments were sub-cloned into GST-encoding pGEX-6P-1 vectors (Amersham, Sweden) using standard molecular techniques. Differentially tagging Pfnek3 to the 6xHis moiety allows for kinase assays involving a few kinases to be examined in detail. Therefore, PCR fragments for TR-*Pfnek3* and TR-ΔPfnek3 were cloned into the 6xHis-encoding pDEST17 vector using Gateway™ technology (Invitrogen, USA). *E. coli* BL21 (DE3) or the CodonPlus™ strain (Stratagene, USA) was electro-transformed with the recombinant plasmids. Using the Rare Codon Analyzer from the University of California (http://www.doe-mbi.ucla.edu/~sumchan/caltor.html), 43 rare codons were found in this 347-residue protein. Of the 43 rare codons found, 29 specifically utilized the rare AUA codon to code for isoleucine. Therefore, attempts were made to express the same genes in CodonPlus™ cells engineered to alleviate codon bias. Successful transformants were induced to express fusion proteins by overnight incubation with 0.5 mM IPTG (isopropyl-beta-D-thiogalactopyranoside) at 22–25 °C. Cells were sonicated (MSE Soniprep, Sanyo) and lysates cleared by centrifugation. Supernatants were affinity-purified with glutathione-sepharose or Ni-NTA according to manufacturer's instructions (Amersham, Sweden; Qiagen, Germany). GST-Pfmap1 and GST-Pfmap2 (gifts from C. Doerig) were expressed similarly in CodonPlus™ cells. In some experiments, recombinant proteins were cleaved of their fusion partner (GST) by incubating for at least three hours at 4 °C with the Precission™ protease (Amersham, Sweden). Eluted proteins were analyzed with SDS–PAGE. Protein expression levels were determined using the Protein Assay Reagent (Bio-Rad, USA). A GST-tagged human MAP kinase (hMAPK1) was purchased from Upstate (USA) for use as a positive control.

2.4. Protein adsorption

To assay for kinase substrate preference, a panel of four polypeptides (pre-diluted to 0.5 mg/ml) was adsorbed to protein-binding 96-well plates (Costar, USA): (i) histone H1, (ii) casein kinase I substrate (peptide sequence RRKDLHDDEEDEAMSITA), (iii) casein kinase II substrate (peptide sequence RRADDSDDDDD; all from Calbiochem, USA) and (iv) dephosphorylated myelin basic protein (MBP; Upstate, USA). Similarly, GST-fusion kinases were also adsorbed for use as substrates for other kinases. Adsorption was achieved by overnight incubation of the proteins in microplate wells at 4 °C in a carbonate buffer (0.15 M sodium carbonate and 0.35 M sodium bicarbonate, pH 9.6). Before use, remaining adsorptive surfaces were blocked with PBS/1% BSA for one hour at room temperature. To control well-to-well consistency of the coated microplates, MBP-coated wells were assayed with hMAPK1 to ensure uniform adsorption. To ascertain equal binding of different GST-tagged kinases to the microplate wells, anti-GST primary antibodies (1:1000 dilution; Sigma, USA) were used to detect adsorbed enzymes, and processed with standard peroxidase-based chemiluminescence to demonstrate uniform adsorption.

2.5. Validation of the ELISA-based kinase assay

Autoradiography is commonly used for protein kinase assays. However, to facilitate future high-throughput inhibitor screens, a chemiluminescent microplate assay was chosen in this study. The performance of the MBP-coated microplates prepared in this study was bench marked against commercially-available ones by adapting the manufacturer's quality control protocol using human MAPK1 (Upstate, USA cat. no. 30-011). To optimize plate reader sensitivity, between 1 and 100 ng of human MAPK1 (per reaction of 30 μl) was tested with a range of ATP concentrations (100–500 μM) to determine whether maximal levels of MBP phosphorylation could be consistently achieved.

2.6. Protein kinase assay

Each kinase reaction mix of 60 μl comprised 10 μg of GST-fusion kinase or the inactive mutant as control, Tris–HCl (50 mM, pH 7.2),

ATP (500 μM), $MgCl_2$ and/or $MnCl_2$ (20 mM and 5 mM, respectively). The kinase mixes were incubated for 30 min at 30 °C. Any phosphorylation activity in the kinase mixes were stopped by adding Laemmli's buffer [18] and denatured at 95 °C for 5 min. The denatured kinase mixes were resolved on 10% SDS–polyacrylamide gels and subjected to the Pro-Q® phosphoprotein gel stain (Invitrogen, USA). The major advantage of the enzyme-linked immunosorbent assay (ELISA) architecture lies in the use of the microplate which is amenable to high-throughput inhibitor screenings. In view of this, 30 μl fractions of the aforesaid kinase mixes were transferred into substrate-coated ELISA microplates immediately after the assembly of the mixtures, to assay their kinase activities. The microplates were simultaneously incubated at 30 °C for 30 min and thereafter quenched by repeated washing with PBS. The quenched microplate kinase assays were blocked for 30 min with PBS/1% BSA and then incubated with mixed monoclonal anti-phosphoserine/threonine antibodies (1:500 dilution; Upstate, USA). The microplate was then subjected to a peroxidase-conjugated secondary antibody (1:4000, Upstate, USA) and the SuperSignal West Femto peroxidase substrate (Pierce, USA). Any resulting chemiluminescence due to the presence of phosphorylated serine and/or threonine residues

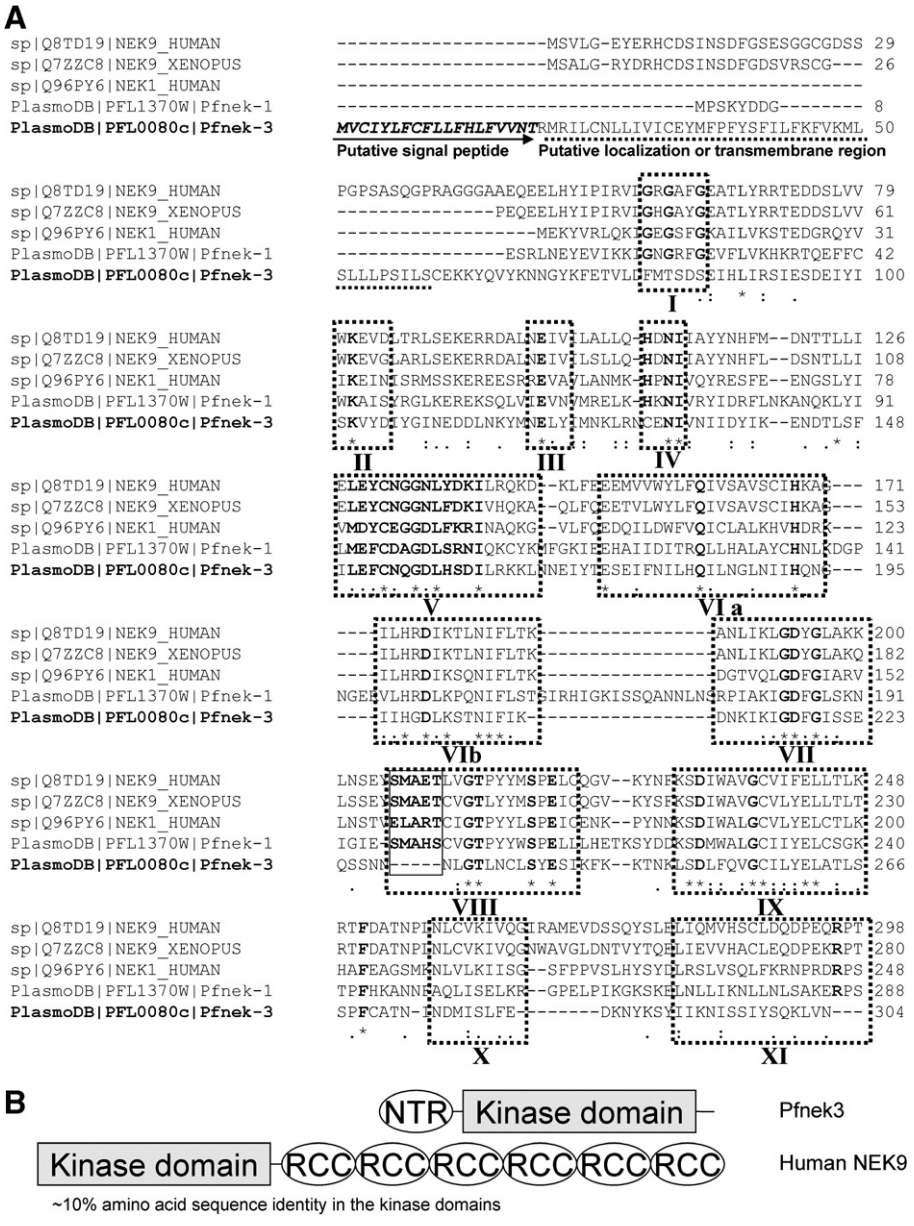

Fig. 1. Sequence alignment of Pfnek3 with other NEKs and comparison of domain architecture with the closest homologue. (A) An N-terminal stretch of 59 primarily hydrophobic residues was predicted to be a signal peptide and organelle-targeting signal or transmembrane region using, respectively, the PlasmoAP, PATS (score: 0.662 of 1) and TMHMM2 algorithms [25–27]. Pfnek3 does not exhibit complete agreement with the 11-subdomain model of eukaryotic protein kinases (indicated with *Roman-numbered boxes*). For example, Pfnek3 belongs to a minority of kinases completely devoid of all three Gs in the glycine triad (GXGXXG) characteristic of subdomain I. Although Pfnek3 lacks the glycine triad (residues 80–85), a lysine residue, potentially important for ATP binding is conserved at K102. Mutation at this residue obliterates the kinase activity of Pfnek3. (B) Schematic diagram of the Pfnek3 domain architecture compared to human NEK9, its closest homologue identified by non-redundant BLASTp searches. Both kinases share a sequence identity of about 10% at their respective kinase domains. The kinase domains were demarcated with the ScanProsite tool at www.expasy.org (Pfnek3: residues 52–334; human NEK9: residues 52–308). A marked divergence of protein architectures is exemplified by Pfnek3 having limited accessory domains. Abbreviations: RCC, Regulator of chromosome condensation domain; NTR, N-terminal region.

was measured using the Genios™ microplate reader (Tecan, Austria). In some experiments, two different GST-fusion kinases were co-incubated in the kinase mixes to detect any in vitro difference in phosphotransfer activity. As controls, either one of the two GST-fusion kinases was replaced with its respective kinase-dead mutant.

2.7. Western blot

As an alternative to the Pro-Q® phosphoprotein gel stain, kinase reactions were performed as described above with the exception that 2.5 μg of MBP was included in the reaction mix as kinase substrate. The mixture was then subjected to SDS–PAGE and transferred to PVDF (polyvinyldifluoride; Millipore, USA) membranes and probed with a monoclonal anti-phosphoserine/threonine antibody mix (Upstate, USA) and visualized by chemiluminescence with a peroxidase-conjugated antibody (Pierce, USA) and the SuperSignal West Femto reagent (Pierce, USA).

2.8. Antibody production

An affinity-purified anti-Pfnek3 antibody was prepared by GeneScript Corp. (New Jersey, USA). Two New Zealand White rabbits were immunized with a synthetic peptide derived from the Pfnek3 amino acid sequence (NQGDLHSDILRKKLC, residues 154–167). The terminal cysteine residue was incorporated to allow coupling to keyhole limpet hemocyanin. The antibody was tested using ELISA and Western blot (WB) prior to fluorescence microscopy. To verify the specificity of anti-Pfnek3, protein-adsorbing microplates were used, as described in *Protein adsorption*, to bind GST-Pfmap2, GST-Pfnek3 or their kinase-inactive mutants. Microplates were probed using a 1:1000 dilution of anti-Pfnek3 and processed for chemiluminescence as described earlier under *Protein kinase assay*. To further verify the specificity of anti-Pfnek3, purified recombinant GST-Pfmap2 and GST-Pfnek3 were subjected to Western blot, as described above, and probed with a 1:1000 dilution of anti-Pfnek3, followed by a peroxidase-conjugated anti-rabbit secondary antibody. Visualization was achieved using a peroxidase substrate, TMB (3,3′,5,5′-tetramethylbenzidine; Sigma, USA).

2.9. Immunofluorescence microscopy

Gradient-centrifugation enriched parasites (both sexual and asexual stages) were smeared, air-dried and fixed on poly-L-lysine slides using 4% paraformaldehyde/PBS. Fixed cells were permeabilized with 0.1% Triton X-100/PBS, and immunolabelled with the affinity-purified Pfnek3 antibody. This was followed by a fluorescein isothiocyanate (FITC)-conjugated anti-rabbit secondary antibody (1:33 dilution; Acris antibodies, Germany). Slides were washed in PBS containing 0.1% Tween 20. DNA was stained with Hoechst 33342 (Invitrogen, USA) at a final concentration of 5 μg/ml. Cover slips were mounted with 90% glycerol in 50 mM Tris (pH 8.0) containing 2.5% (w/v) 1,4-diazabicyclo[2.2.2]octane (Sigma, USA) and viewed with an Olympus BX60 fluorescence microscope with the same microscope and camera settings for images stained with the same fluorophore.

3. Results and discussion

3.1. Bio-computational identification of Pfnek3

The predicted ORF of Pfnek3 encodes a protein with limited homology of about 10% sequence identity at its kinase domain to its closest NEK family member, human NEK9, identified by BLASTp searches (Fig. 1). This was carried out independently and agrees with the biocomputational data of [19]. The information contrasted against a phylogenetic tree plotted using ClustalW which placed Pfnek3 in a different clade from mammalian NEKs (Fig. 2). In comparison to the first malarial NEK reported (Pfnek1), Pfnek3 is hardly similar in terms of residue composition (17% identity) and peptide length (1057 and 347 amino acids, respectively). Close scrutiny of the alignment data revealed a few peculiarities which may explain the uniqueness of Pfnek3 (Fig. 1). Firstly, the major region of similarity with human NEK9 is embedded only in the kinase domain. Secondly, a putative N-terminal signal sequence and localization signal or transmembrane region in Pfnek3 predicted by the PlasmoAP, PATS and TMHMM2 algorithms, respectively, may give an indication of an unknown cellular localization. Thirdly, Pfnek3 appears to be devoid of any kinase activation motif commonly located at subdomain VIII (Fig. 1). Collaterally, Pfnek1 lacks the classical NIMA activation motif, FXXT, at subdomain VIII which was replaced by a SMAHS motif reminiscent of a MEK activation site [12] (included in Fig. 1 for comparison). Interestingly, Pfnek3 lacks

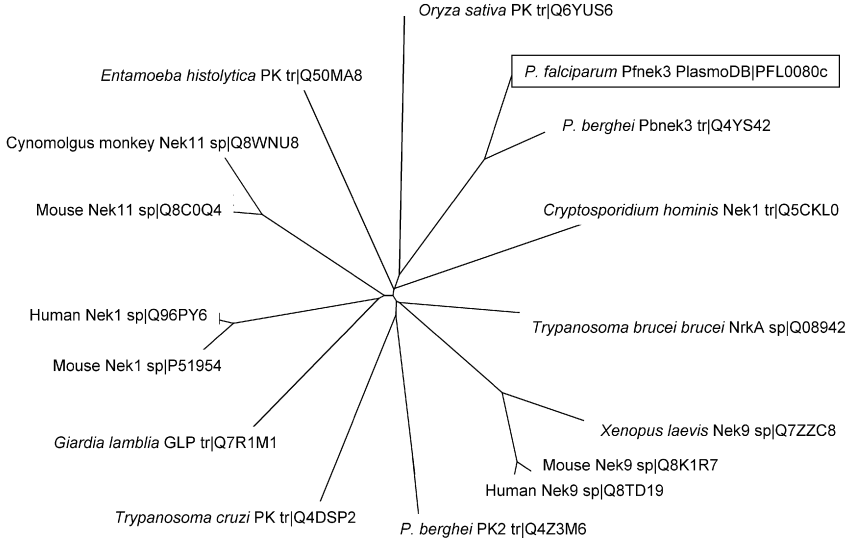

Fig. 2. Phylogenetic analysis. The full-length Pfnek3 amino acid sequence was used to query the Swiss-Prot and TrEMBL non-redundant generalist databases via BLASTp program at the Expasy website (www.expasy.org). Incompletely annotated sequences were filtered out and the remaining sequences were extracted and submitted to the ClustalW sequence alignment package, which generated alignment dendrograms viewed with the TreeView program (http://taxonomy.zoology.gla.ac.uk/rod/treeview.html). The dendrogram detaches Pfnek3, as well as the rodent malarial homologue (Pbnek2) from mammalian NEKs. *Abbreviations*: PK, protein kinase; sp, Swiss-Prot database sequence identifier; tr, TrEMBL database sequence identifier.

both the FXXT and SMAHS motifs (Fig. 1, subdomain VIII). Other than differences of functional motifs, there are other molecular differences between Pfnek3 and other NEKs. For example, the 11 sub-domains of the protein kinase catalytic domain encoded by the ORF of Pfnek3 were not completely in agreement with known NEKs [20]. Sub-domain I does not contain the glycine triad (GXGXXG) principally involved in ATP binding. Instead, the corresponding motif is altered to FMTSDS in Pfnek3, with none of the Gs in the triad conserved (Fig. 1). Reportedly, nearly a third of human protein kinases lacks the third G of the triad, and 11% lack the first one [21]. So far, a small collection of kinases, for example, *Schizosaccharomyces pombe* MIK1, are reportedly devoid of all three Gs but retain protein kinase activity [22], and this may now include Pfnek3. Also, the highly conserved lysine residue in sub-domain II that is critical to contacting, anchoring and orienting the α- and β-phosphates of ATP could not be detected initially using PROSITE algorithms. However, based on multiple sequence alignments with other protein kinases, it was putatively identified as K102. Intriguingly, the residues in the vicinity of K102 in Pfnek3 (Fig. 1) have deviated from consensus sequences reported in other NIMA-related kinases [20]. Furthermore, the HRDXXXXN base-acceptor motif of eukaryotic protein kinases in sub-domain VIb is represented by a different motif, HGDLKSTN. Since the frequency of a glycine appearing in this sub-domain among eukaryotic protein kinases is believed to be low [20], this particular glycine (G199) serves as an interesting target, therefore, warranting further studies on its role. Finally, the aspartate residue conserved in the DFG motif of sub-domain VII (D217), is thought to elicit the binding of Mg^{2+}or Mn^{2+} ion associated with the β- and γ-phosphates of ATP. And since the Pfnek3 sequence

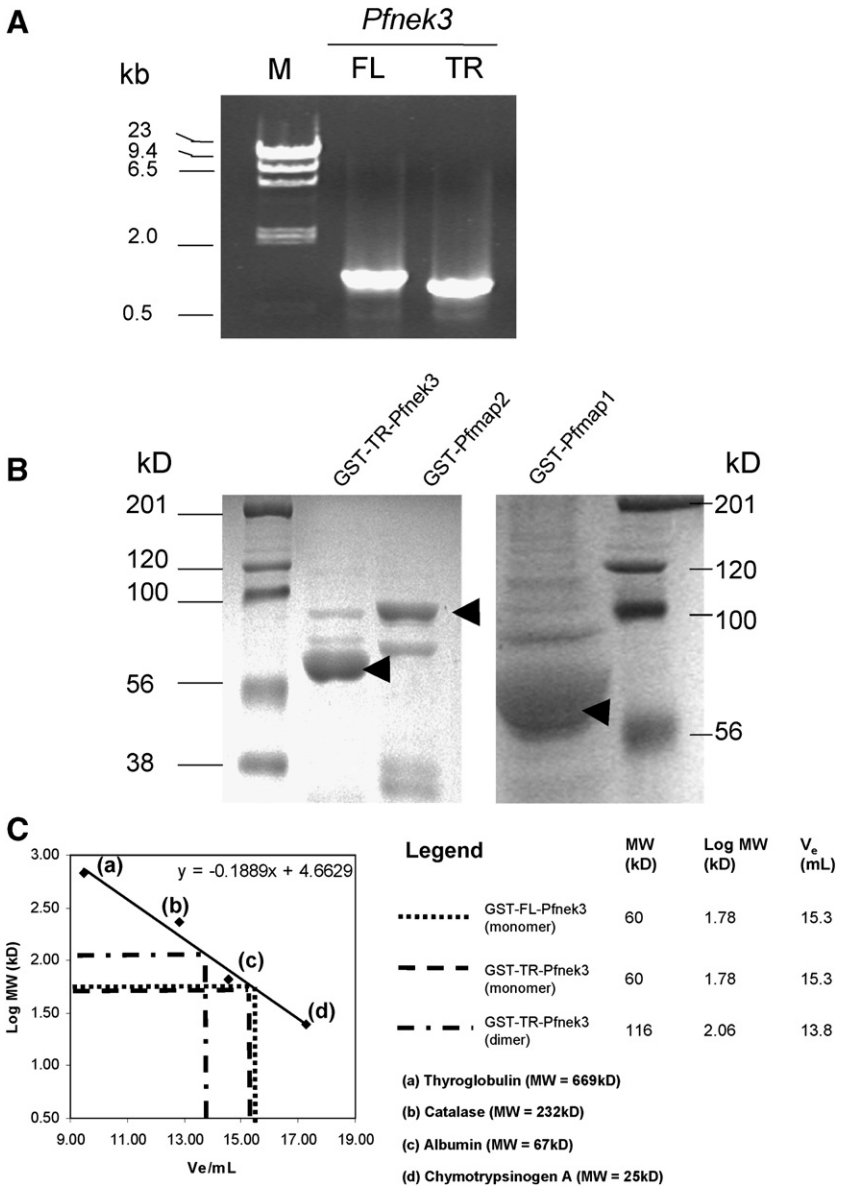

Fig. 3. Molecular cloning and recombinant expression of Pfnek3. (A) M = λ/*Hin*dIII molecular weight markers. FL: FL-Pfnek3 amplification product. TR: TR-Pfnek3 amplification product. (B) Expression of GST-tagged kinases. (C) Analysis of purified GST-FL-Pfnek3 and GST-TR-Pfnek3 via analytical gel filtration indicates enriched fractions of monomers of about 60 kD.

contains the PROSITE protein kinase signature IIHGDLKSTNIF (PROSITE identifier: PS00108), this aspartate residue is believed to be similarly involved in phosphotransfer catalysis.

3.2. Molecular cloning of FL- and TR-Pfnek3

The *Pfnek3* ORF was amplified using either cDNA or genomic DNA from *P. falciparum* Tan or 3D7 strains as template, and the amplified product size appeared identical (~1 kb) suggesting that the *Pfnek3* gene is non-intronic, as was later confirmed by DNA sequencing. The Pfnek3 DNA sequence from the 3D7 strain varied from the Tan stain at a single base (A → C at nucleotide 975). The Tan strain Pfnek3 DNA was retained for further work. The cloning of a truncated Pfnek3 (TR-Pfnek3; Fig. 3A) was necessitated by the fact that the 59-residue hydrophobic N-terminal domain of the full-length version (FL-Pfnek3), which was predicted to be a signal peptide or an organelle-targeting signal (indicated in Fig. 1) and therefore interfere with the solubility of the expressed recombinant protein. The conceptually-translated FL-Pfnek3 is 347 amino acids long and SDS–PAGE indicated that the GST-fusion protein was approximately 60 kD (Fig. 3B). Analytical gel filtration of FL- and TR-Pfnek3 revealed that recombinant Pfnek3 existed primarily as monomers of molecular weights similar to that on SDS–PAGE gels (Fig. 3C).

3.3. Kinase activity of recombinant Pfnek3

The ELISA-based kinase assay has been benchmarked against commercial systems as described in Section 2. To investigate whether the sequence divergence of Pfnek3 from mammalian NEK family members is reflected by its functional properties, kinase assays were performed with a panel of substrates and cofactors (Fig. 4). Catalytic activity of recombinant Pfnek3 was assayed using four compounds as kinase substrates: (i) MBP, (ii) histone H1, (iii) casein kinase I peptide substrate (CKS I) and (iv), casein kinase II peptide substrate (CKS II). Biochemical data indicated that Pfnek3 satisfactorily phosphorylates an artificial substrate MBP but not histone H1 nor casein kinase peptide substrates (Fig. 4A). This in vitro substrate preference is dissimilar to that of mammalian NEKs since recombinant mammalian NEKs uses α- or β-casein but less commonly MBP as a substrate. Hence, the in vitro substrate preference of Pfnek3 is consistent with the distant relationship of this enzyme to mammalian NEKs. Contrasting to most mammalian NEKs, Pfnek3 was a more efficient kinase when supplied with manganese as co-factor instead of magnesium (Fig. 4B). When a buffer containing both co-factors was used, there was no increase in MBP phosphorylation, indicating that the presence of manganese was sufficient.

TR-Pfnek3, but not the full-length enzyme, demonstrated kinase activities at levels of three- to eight-folds versus controls using an equal amount of bacterially-expressed GST in place of GST-TR-Pfnek3 (Fig. 4B). To verify that the phosphotransfer onto MBP was indeed mediated by Pfnek3 and not by co-purified bacterial kinases, a mutant TR-Pfnek3 carrying a K102M substitution at its ATP-binding motif was generated (ΔPfnek3) and shown to lack kinase activity (Fig. 4B).

To elucidate the effect of the putative signal sequence on downstream kinase assays, activity of the full-length protein was also determined. GST-FL-Pfnek3 did not exhibit detectable kinase activities (Fig. 4C). If the N-terminal domain is erroneously predicted as a signal sequence, this data may implicate the N-terminal domain in playing a self-regulatory function, akin to PfPKB, where its N-terminal domain is demonstrated to modulate catalytic activity [23]. To elucidate its intricate mechanisms would probably require independent and separate structural studies akin to studies of a kinase

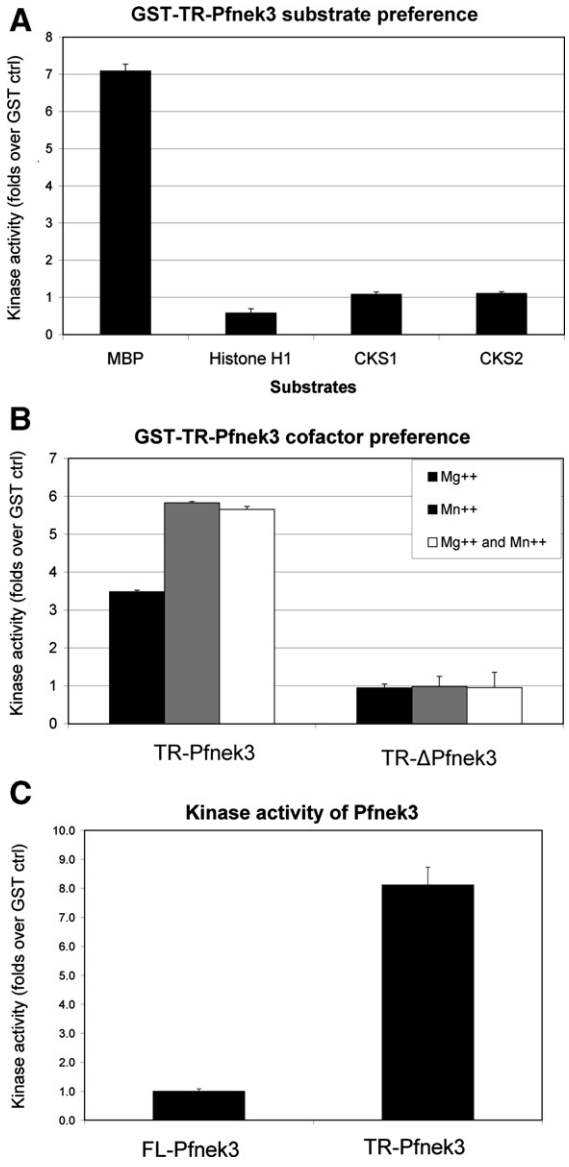

Fig. 4. Factors affecting Pfnek3 kinase activity. (A) Substrate preference screening of recombinant truncated (TR) Pfnek3 reveals a preference for myelin basic protein (MBP) in the co-presence of magnesium and manganese. (B) Kinase activities of GST-TR-Pfnek3 and its 'kinase-dead' mutant in the presence of Mg^{++} and/or Mn^{++} reveals a preference for Mn^{++} as cofactor when MBP was used as substrate. Substrates used were MBP (dephosphorylated myelin basic protein), CKSI (casein kinase I substrate), CKSII (casein kinase II substrate) and histone H1. (C) The kinase activity of recombinant FL-Pfnek3 is suppressed by the presence of an N-terminal putative signal sequence and organelle-targeting signal and/or transmembrane region. Kinase activities are expressed as "*fold over GST ctrl*" for the purpose of normalizing batch-to-batch assays. A GST control consisted of adsorbed substrates assayed with bacterially-expressed GST to establish background phosphorylation.

named *twitchin*, which was rendered inactive due to the presence of an autoinhibitory peptide sequence [24]. To show that the fusion partner (GST) did not affect kinase activity, wild-type GST-Pfnek3 was cleaved of its fusion partner and subjected to the same kinase assay, with comparable results as the fusion proteins (not shown).

3.4. Pfnek3 directionally phosphorylates Pfmap2

The transcription profile of Pfnek3 revealed high gametocyte expression levels akin to Pfmap2, a gametocyte-specific MAPK [9]. To investigate the possibility of any Pfnek3–Pfmap2 interaction, the phosphorylation statuses of both enzymes under identical conditions were examined. The

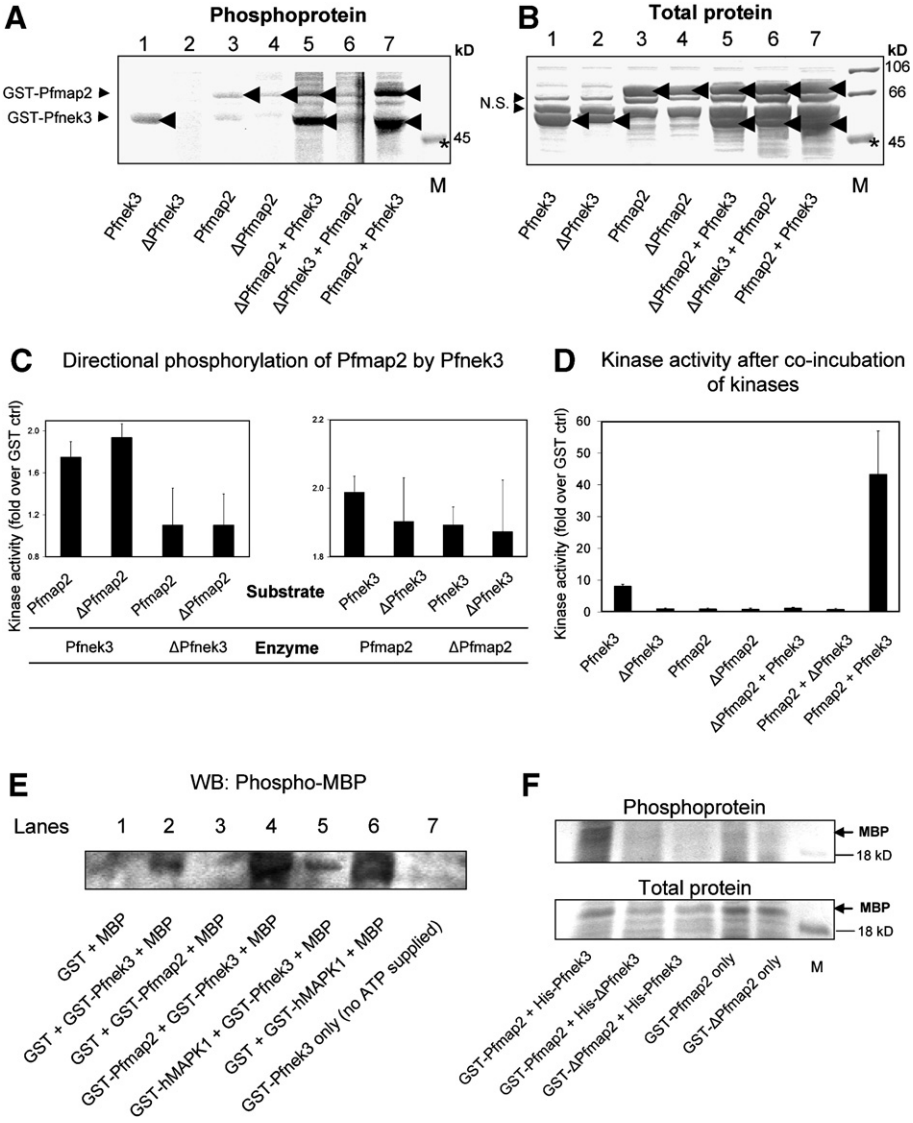

Fig. 5. Pfnek3 phosphorylates Pfmap2 and stimulates its kinase activity. (A) GST-TR-Pfnek3 alone existed as a basally phosphorylated protein (Lane 1). The presence of either catalytically-active or inactive GST-Pfmap2 caused an increase in GST-TR-Pfnek3 autophosphorylation (Lanes 5 and 7). GST-TR-Pfnek3 was capable of phosphorylating GST-Pfmap2 (Lane 7). (B) The same gel in (A) stained with the EZ-blue® high-sensitivity total protein stain (Sigma, USA) indicates uniform loading of the same protein in each well. M = Peppermintstick® molecular weight markers (Invitrogen, USA). The 45 kD band (indicated with an asterisk) corresponds to a known phosphoprotein visible with both the Pro-Q® phosphoprotein (Invitrogen, USA) and EZ-blue®stains. The 66 and 106 kD bands (non-phosphoproteins) are only visible when stained with a total protein stain. NS = Non-specific protein bands ubiquitous in GST-purification preparations. (C) The phosphorylation of GST-Pfmap2 by GST-TR-Pfnek3 was confirmed using ELISA. GST-Pfmap2, GST-TR-Pfnek3 or their inactive mutants were adsorbed to microplates as described in Section 2 and used as substrate for another kinase. The values are expressed as folds over bacteria-expressed GST controls. (D) Fractions of the kinase mixes used in (A) were transferred to MBP-coated microplates immediately after the addition of ATP and processed for chemiluminescence as described in Section 2. The co-incubation of GST-TR-Pfnek3 and GST-Pfmap2 produced a markedly increased kinase activity. The replacement of any one of the two kinases with a kinase-inactive mutant abolished the increased kinase activity. (E) The observation in (D) was confirmed by probing for phospho-MBP using Western blots (Lane 4). Replacing GST-Pfmap2 with GST-hMAPK1 did not produce the same result, suggesting that the Pfmap2–Pfnek3 interaction is specific (Lane 5). (F) To assess the kinase activity of GST-Pfmap2 alone after co-incubation with His-TR-Pfnek3, the kinase reaction mix was applied through a Ni-NTA column to ensure removal of His-TR-Pfnek3 and uniform loading of GST-Pfmap2 or its mutant in all lanes, as verified by SDS–PAGE (not shown). MBP was added to the eluate and incubated for another 30 min at 30 °C. The mixture was subjected to SDS–PAGE and subjected to both phosphoprotein and total protein stains as was performed for (A) and (B). M = Peppermintstick® protein standards (Invitrogen, USA).

approach was based on the use of a gel-based phosphoprotein stain coupled to the ELISA microplate so that congruent results can be derived.

Since the N-terminal-deleted copy of Pfnek3 was catalytically active (Fig. 4C), it was used in subsequent experiments involving kinase co-incubations. Gel-based phosphoprotein staining indicated that GST-TR-Pfnek3 was able to phosphorylate Pfmap2 (Fig. 5A). When ΔPfnek3 was used in place of the wildtype enzyme, the observation of increased phosphorylation on Pfmap2 was abolished. This implied that GST-TR-Pfnek3, and not bacterial kinases, was responsible for phosphorylating GST-Pfmap2. This observation was corroborated by coating microplates with GST-Pfmap2 and using it as a substrate for GST-TR-Pfnek3 (Fig. 5C). Uniformity in the amount of adsorbed proteins was verified using anti-GST antibodies versus blank-coated control wells (not shown). We observed that GST-TR-Pfnek3, but not GST-ΔPfnek3, was able to increase the phosphorylation state of Pfmap2 in ELISA assays (Fig. 5C). The reaction between Pfnek3 and Pfmap2 was reciprocally performed and there was no significant difference between the phosphorylation statuses of Pfnek3 incubated with either Pfmap2 or ΔPfmap2 (Fig. 5C). Therefore, the phosphorylation of Pfmap2 by Pfnek3 is directional.

3.5. Pfnek3 stimulates Pfmap2 kinase activity

To assay for the effect of Pfnek3 on Pfmap2 kinase activity, fractions from the samples of kinase mixes destined for the gel-based assay were transferred into MBP-coated ELISA plates concurrently. MBP has been reported to be a suitable substrate for Pfmap2 [4]. Using this assay format, GST-Pfmap2 alone did not detectably phosphorylate MBP (Fig. 5D) vis-à-vis radioactive kinase assays [4]. Surprisingly, when GST-Pfmap2 was co-incubated with GST-Pfnek3, the levels of MBP phosphorylation were higher than the summation of the individual kinase activities (Fig. 5D). To eliminate the possibility that the observed phosphorylation was due to contamination of bacterial kinases or the GST moiety, GST-ΔPfnek3 or GST-ΔPfmap2 was added to reaction mixtures containing GST-Pfmap2 or GST-Pfnek3, respectively. In these controls, there was no increase in MBP phosphorylation (Fig. 5D). To support this observation, the experiment was repeated using Western blot and probed for phospho-MBP with similar conclusions (Fig. 5E). To further demonstrate the notion that Pfnek3 activates Pfmap2, GST-Pfmap2 was co-incubated with His-TR-Pfnek3. The latter kinase was removed via nickel affinity chromatography and the separated GST-Pfmap2 demonstrated enhanced MBP phosphorylation over controls containing either GST-ΔPfmap2 or His-TR-ΔPfnek3 (Fig. 5F). As demonstrated by experiments with catalytically-inactive mutant enzymes, enhanced MBP phosphorylation was dependent on the kinase activities of both Pfnek3 and Pfmap2. However, when both kinases were co-incubated, ELISA and gel-based assays indicated that the phosphorylation of Pfmap2 by Pfnek3 was directional. This suggests that Pfnek3 may be upstream of Pfmap2 in a kinase cascade, at least in vitro.

3.6. Pfnek3 autophosphorylates in the presence of Pfmap2, active or inactive

We noted with interest that the presence of Pfmap2 or ΔPfmap2 was sufficient to cause an increase in phosphorylation on Pfnek3 versus samples containing Pfnek3 only (Fig. 5A), but does not possess detectable kinase activity alone (Fig. 5D). Because both Pfmap2 and ΔPfmap2 did not detectably phosphorylate Pfnek3 (Fig. 5C) and did not demonstrate catalytic activity (Fig. 5D–E), it is possible that Pfnek3 autophosphorylates in the presence of Pfmap2. The reason for this is not entirely clear. Nevertheless, this observation indirectly strengthens the postulation that the markedly increased kinase activity of co-incubated Pfmap2 and Pfnek3 (Fig. 5D) was due to the activity of Pfmap2 stimulated by Pfnek3, and not due to the kinase activity of autophosphorylated Pfnek3 alone.

3.7. Pfnek3 stimulates Pfmap2 but not Pfmap1 or hMAPK1

To investigate whether the effect is specific to Pfmap2 and not other kinases, the same experiments were repeated with two other kinases, where human MAPK1 (hMAPK1) or GST-Pfmap1 was co-incubated with GST-Pfnek3 in a similar fashion. Contrastingly, the incubation of GST-Pfnek3 with hMAPK1 resulted in significantly-decreased MBP phosphorylation levels (Fig. 6A). This was also observed in Western blot experiments (Fig. 5E). To exclude the possibility that GST-FL-Pfnek3 and GST-TR-Pfnek3 might also be substrates of GST-hMAPK1, resulting in ATP exhaustion, the concentration of ATP was increased from 100 to 500 μM in subsequent experiments. However, the availability of excess ATP did not result in increased MBP phosphorylation (not shown). Moreover, to verify that the lack of MBP phosphorylation was not due to insufficient incubation time, the incubation period was ex-

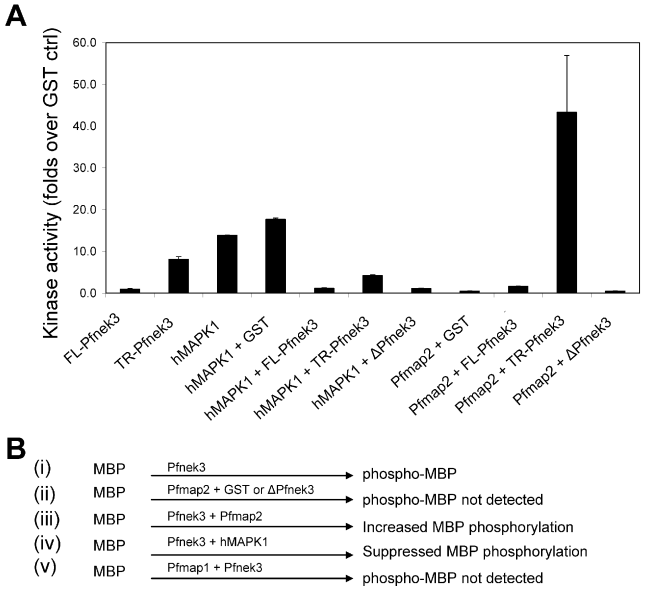

Fig. 6. Pfnek3 activates Pfmap2 but not hMAPK1. (A) GST-TR-Pfnek3, when co-incubated with GST-Pfmap2 results in increased phosphorylation of MBP. When GST-TR-Pfnek3 was replaced with bacterially-expressed GST, GST-FL-Pfnek3 or GST-ΔPfnek3, this phenomenon was not observed. To show that the enhancement in (A) is specific to GST-Pfmap2, GST-Pfnek3 and its variants were co-incubated with hMAPK1. Enhancements to kinase activity were not observed. (B) Summary of data from co-incubation assays. (i) GST-TR-Pfnek3 is an active kinase in the presence of Mn^{2+}using MBP as substrate. (ii) GST-Pfmap2 exhibits little or no activity using this assay format. (iii) Adding GST-Pfmap2 to GST-TR-Pfnek3 enhanced MBP phosphorylation. (iv) As control, adding another kinase (hMAPK1) to GST-Pfnek3 counteracts MBP phosphorylation, hence suggesting that the phenomenon of Pfnek3 stimulating Pfmap2 is not artefactual. (v) GST-Pfmap1 was inert with GST-Pfnek3.

tended from 30 to 90 min with no detectable difference in activity (not shown). Next, to verify that the suppression of MBP phosphorylation was not an artifact arising from the presence of another free protein in excessive concentrations, GST-hMAPK1 was co-incubated with bacterially-expressed GST diluted to match the in vitro concentrations of GST-FL-Pfnek3 and GST-TR-Pfnek3. GST did not inhibit GST-hMAPK1 (Fig. 6A). Moreover, when GST was replaced with ΔPfnek3, the inhibitory effect remained intact (Fig. 6A).

To test whether GST-Pfnek3 has any role in regulating a typical *Plasmodium* MAPK, GST-Pfmap1, the same kinase co-incubation experiments were constructed. Despite being solubly expressed (Fig. 3B), GST-Pfmap1 exhibited undetectable in vitro kinase activity using different assay conditions in this and other laboratories (C. Doerig, personal communication) contrary to a previous report of activity [3]. Additionally, GST-Pfnek3 was unable to activate GST-Pfmap1 in this study. A schematic summary of the results is recapitulated in Fig. 6B.

3.8. Expression of endogenous Pfnek3

Although microarray data indicate predominant transcriptional activity of Pfnek3 during the gametocyte stage [9], actual translational and subcellular localization information remains unknown. This is especially important since the presence of a putative signal sequence in Pfnek3 suggested intracellular protein transportation. With these questions in mind, antibodies to Pfnek3 were raised (Fig. 7A) and immunofluorescence assays enabled the confirmation of the transcriptome data of Le Roch et al. [9] with regards to gametocyte-stage Pfnek3 expression (Fig. 7B). Moreover, expression was also detected in the late stages of asexual intraerythrocytic parasites, despite no observable distinct patterns of localization.

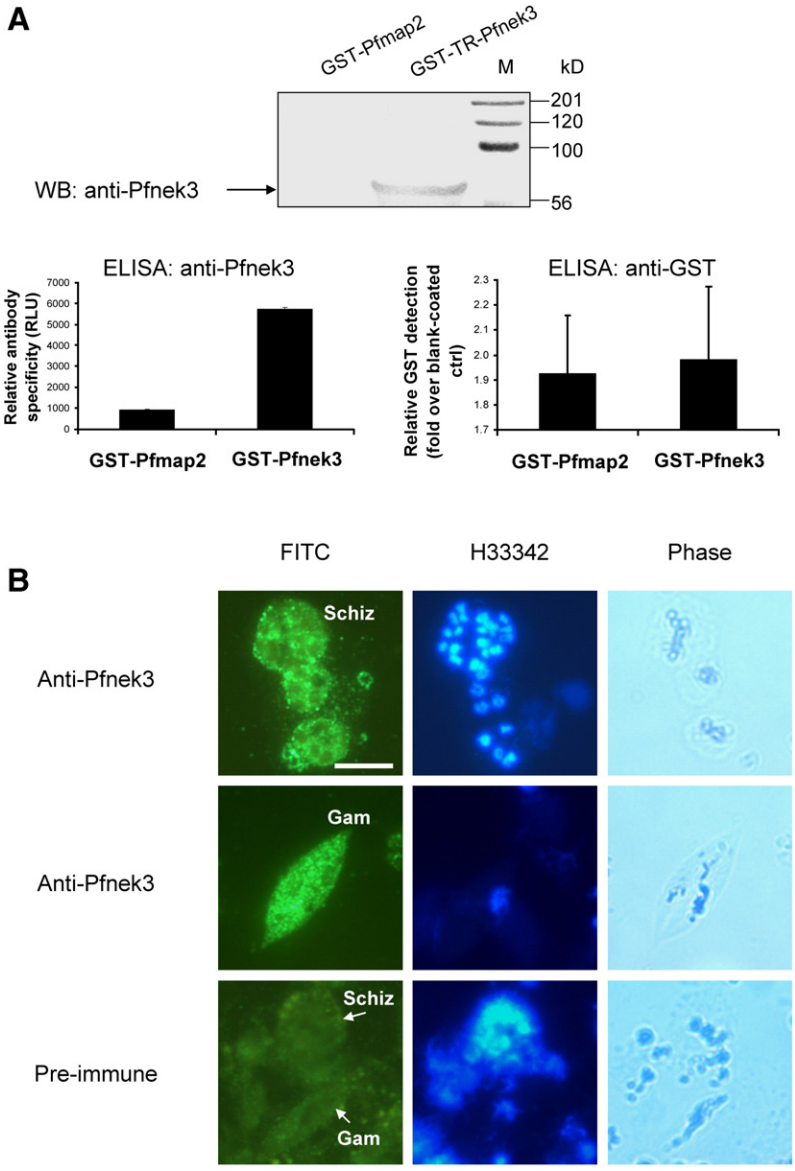

Fig. 7. Endogenous expression of Pfnek3. (A) Specificity of anti-Pfnek3 antibody was verified with Western blots and ELISA, as described under Section 2. Scale bar represents 10 μm. (B) Schizonts (schiz) and gametocytes (gam) were positively-stained with anti-Pfnek3. Co-staining with Hoechst 33342 confirms the presence of parasite nuclei.

4. Conclusions

Pfnek3 was demonstrated by microarray data to be highly expressed in the gametocyte [9], and our immunofluorescence detection confirms the same. Hence, Pfnek3 may be a possible activator present in the gametocyte extract used to stimulate Pfmap2 in an earlier study [4]. Contrastingly, this enhancement was not observed when Pfmap2 was substituted by a hMAPK1 or Pfmap1, indicating the presence of a kinase-specific interaction. Nevertheless, in vivo systems will have to be constructed to further characterize their physiological roles in the gametocyte.

Given that Pfnek3 is divergent from mammalian NEKs, there is potential for Pfnek3 as a candidate drug target with parasite-selective toxicity, provided the disruption of this gene can be shown to hamper parasite development. To support this endeavor, the microplate-based kinase inhibition assays are poised strategically for high-throughput screening of compound libraries, with lead compounds subsequently analyzed for their effects on parasite growth. Most importantly, the biochemical effects of Pfnek3 on various MAPKs may suggest an unusual mode of eukaryotic MAPK interaction with an atypical member of the NIMA kinase family in the *Plasmodium* parasite.

Acknowledgements: The authors are indebted to Dr. Christian Doerig for providing the plasmids carrying Pfmap1 and Pfmap2. Dr. Doreen Tan invaluably assisted during immunofluorescence analyses and provided useful critique. Technical expertise for analytical gel filtration was sought from Mr. Lam Kin Wai. We thank MR4 for providing us with malaria parasites contributed by D.J. Carucci. This study was funded by an A*-BMRC grant R182-000-061-305 administered by the National University of Singapore.

References

[1] Martens, P. and Hall, L. (2000) Malaria on the move: human population movement and malaria transmission. Emerg. Infect. Dis. 6, 103–109.
[2] Leete, T.H. and Rubin, H. (1996) Malaria and the cell cycle. Parasitol. Today 12, 442–444.
[3] Graeser, R., Kury, P., Franklin, R.M. and Kappes, B. (1997) Characterization of a mitogen-activated protein (MAP) kinase from *Plasmodium falciparum*. Mol. Microbiol. 23, 151–159.
[4] Dorin, D., Alano, P., Boccaccio, I., Ciceron, L., Doerig, C., Sulpice, R., Parzy, D. and Doerig, C. (1999) An atypical mitogen-activated protein kinase (MAPK) homologue expressed in gametocytes of the human malaria parasite *Plasmodium falciparum*. Identification of a MAPK signature. J. Biol. Chem. 274, 29912–29920.
[5] Rangarajan, R., Bei, A.K., Jethwaney, D., Maldonado, P., Dorin, D., Sultan, A.A. and Doerig, C. (2005) A mitogen-activated protein kinase regulates male gametogenesis and transmission of the malaria parasite *Plasmodium berghei*. EMBO Rep. 6, 464–469.
[6] Khan, S.M., Franke-Fayard, B., Mair, G.R., Lasonder, E., Janse, C.J., Mann, M. and Waters, A.P. (2005) Proteome analysis of separated male and female gametocytes reveals novel sex-specific *Plasmodium* biology. Cell 121, 675–687.
[7] Ward, P., Equinet, L., Packer, J. and Doerig, C. (2004) Protein kinases of the human malaria parasite *Plasmodium falciparum*: the kinome of a divergent eukaryote. BMC Genomics 5, 79.
[8] Bozdech, Z., Llinas, M., Pulliam, B.L., Wong, E.D., Zhu, J. and DeRisi, J.L. (2003) The transcriptome of the intraerythrocytic developmental cycle of *Plasmodium falciparum*. PLoS Biol. 1, E5.
[9] Le Roch, K.G., Johnson, J.R., Florens, L., Zhou, Y., Santrosyan, A., Grainger, M., Yan, S.F., Williamson, K.C., Holder, A.A., Carucci, E.A., Yates 3rd, J.R. and Winzeler, E.A. (2004) Global analysis of transcript and protein levels across the *Plasmodium falciparum* life cycle. Genome Res. 14, 2308–2318.
[10] Osmani, S.A., Pu, R.T. and Morris, N.R. (1988) Mitotic induction and maintenance by overexpression of a G2-specific gene that encodes a potential protein kinase. Cell 53, 237–244.
[11] O'Connell, M.J., Krien, M.J. and Hunter, T. (2003) Never say never. The NIMA-related protein kinases in mitotic control. Trends Cell Biol. 13, 221–228.
[12] Dorin, D., Le Roch, K., Sallicandro, P., Alano, P., Parzy, D., Poullet, P., Meijer, L. and Doerig, C. (2001) Pfnek-1, a NIMA-related kinase from the human malaria parasite *Plasmodium falciparum*: biochemical properties and possible involvement in MAPK regulation. Eur. J. Biochem. 268, 2600–2608.
[13] Dorin, D., Semblat, J.P., Poullet, P., Alano, P., Goldring, J.P., Whittle, C., Patterson, S., Chakrabarti, D. and Doerig, C. (2005) PfPK7, an atypical MEK-related protein kinase, reflects the absence of classical three-component MAPK pathways in the human malaria parasite *Plasmodium falciparum*. Mol. Microbiol 55, 184–196.
[14] Chan, M. and Sim, T.S. (2005) Functional analysis, overexpression, and kinetic characterization of pyruvate kinase from *Plasmodium falciparum*. Biochem. Biophys. Res. Commun. 326, 188–196.
[15] Dyson, M.R., Shadbolt, S.P., Vincent, K.J., Perera, R.L. and McCafferty, J. (2004) Production of soluble mammalian proteins in *Escherichia coli*: identification of protein features that correlate with successful expression. BMC Biotechnol. 4, 32.
[16] Chan, M. and Sim, T.S. (2003) Recombinant *Plasmodium falciparum* NADP-dependent isocitrate dehydrogenase is active and harbours a unique 26 amino acid tail. Exp. Parasitol. 103, 120–126.
[17] Ho, S.N., Hunt, H.D., Horton, R.M., Pullen, J.K. and Pease, L.R. (1989) Site-directed mutagenesis by overlap extension using the polymerase chain reaction. Gene 77, 51–59.
[18] Laemmli, U.K. (1970) Cleavage of structural proteins during the assembly of the head of bacteriophage T4. Nature 227, 680–685.
[19] Reininger, L., Billker, O., Tewari, R., Mukhopadhyay, A., Fennell, C., Dorin-Semblat, D., Doerig, C., Goldring, D., Harmse, L., Ranford-Cartwright, L., Packer, J. and Doerig, C. (2005) A NIMA-related protein kinase is essential for completion of the sexual cycle of malaria parasites. J. Biol. Chem. 280, 31957–31964.
[20] Hanks, S.K. and Hunter, T. (1995) Protein kinases 6. The eukaryotic protein kinase superfamily: kinase (catalytic) domain structure and classification. Faseb J. 9, 576–596.
[21] Kostich, M., English, J., Madison, V., Gheyas, F., Wang, L., Qiu, P. et al., (2002) Human members of the eukaryotic protein kinase family. Genome Biol. 3, research0043.1–0043.12.
[22] Lee, M.S., Enoch, T. and Piwnica-Worms, H. (1994) mik1+ encodes a tyrosine kinase that phosphorylates p34cdc2 on tyrosine 15. J. Biol. Chem. 269, 30530–30537.
[23] Kumar, A., Vaid, A., Syin, C. and Sharma, P. (2004) PfPKB, a novel protein kinase B-like enzyme from *Plasmodium falciparum*: I. Identification, characterization, and possible role in parasite development. J. Biol. Chem. 279, 24255–24264.
[24] Hu, S.H., Parker, M.W., Lei, J.Y., Wilce, M.C., Benian, G.M. and Kemp, B.E. (1994) Insights into autoregulation from the crystal structure of twitchin kinase. Nature 369, 581–584.
[25] Foth, B.J., Ralph, S.A., Tonkin, C.J., Struck, N.S., Fraunholz, M., Roos, D.S., Cowman, A.F. and McFadden, G.I. (2003) Dissecting apicoplast targeting in the malaria parasite *Plasmodium falciparum*. Science 299, 705–708.
[26] Zuegge, J., Ralph, S., Schmuker, M., McFadden, G.I. and Schneider, G. (2001) Deciphering apicoplast targeting signals – feature extraction from nuclear-encoded precursors of *Plasmodium falciparum* apicoplast proteins. Gene 280, 19–26.
[27] Krogh, A., Larsson, B., von Heijne, G. and Sonnhammer, E.L. (2001) Predicting transmembrane protein topology with a hidden Markov model: application to complete genomes. J. Mol. Biol. 305, 567–580.